



A tracer study in an Alaskan gravel beach and its implications on the persistence of the Exxon Valdez oil

Hailong Li^{a,b,*}, Michel C. Boufadel^{b,*}

^a School of Water Resources and Environmental Science, China University of Geosciences-Beijing, Beijing 100083, PR China

^b Dept. of Civil and Environmental Engineering, Temple University, 1947 N. 12th Street, Philadelphia, PA 19122, USA

ARTICLE INFO

Keywords:

Oil-spills
Tracer study
Tidal beach
Bioremediation
Nutrient application
Seawater-groundwater interaction

ABSTRACT

Despite great efforts including bioremediation, the 1989 Exxon Valdez oil spills persist in many gravel beaches in Prince William Sound, Alaska, USA. To explore this mystery, a lithium tracer study was conducted along two transects on one of these beaches. The tracer injections and transports were successfully simulated using the 2-dimensional numerical model MARUN. The tracer stayed much longer in the oil-persisting, right transect (facing landward) than in the clean, left transect. If the tracer is approximately regarded as oils, oils in the upper layer would have more opportunities to enter the lower layer in the right transect than in the left one. This may qualitatively explain the oil persistence within the right transect. When the tracer is regarded as nutrients, the long stay of nutrients within the right transect implies that the oil persistence along the right transect was not due to the lack of nutrients during the bioremediation.

© 2011 Elsevier Ltd. All rights reserved.

1. Introduction

In March 1989 the Exxon Valdez spill of about 41 million liters of Alaskan North Slope crude oil polluted ~800 km of rocky intertidal shorelines within Prince William Sound, Alaska (Bragg et al., 1994; Neff et al., 1995). Despite of the great efforts of remediation immediately following the spill and the large-scale bioremediation projects conducted in summers from 1989 to 1992 (Bragg et al., 1994; Taylor and Reimer, 2008), subsurface oil residues persist on many initially-polluted beaches (Hayes and Michel, 1999; Li and Boufadel, 2010; Owens et al., 2008; Short et al., 2007, 2004, 2006; Taylor and Reimer, 2008; Xia et al., 2010). In 2001 oil residues were found on 78 of 91 beaches randomly selected according to the oiling history (Short et al., 2004). With annualized loss rates decreasing from ~68% yr⁻¹ before 1992 to ~4% yr⁻¹ after 2001, weathering processes are slowed in sediments, and retention of toxic polycyclic aromatic hydrocarbons is prolonged (Michel and Hayes, 1999; Short et al., 2007).

In a study conducted on a gravel beach (EL-056C, see Fig. 1) located at (147° 34' 17.42" W, 60° 33' 45.57" N), Li and Boufadel (2010) found that the beach is made up of two layers: an upper layer of loose and coarse material with a very large hydraulic conductivity underlain by a layer with fine material whose hydraulic

conductivity is around 1000 folds smaller. Their findings corroborated the general structure of beaches in mid- and high-latitude regions (Davies, 1980; Hayes, 1967; Owens et al., 2008). They also found that the elevation of the water table during low tide with respect to the interface of the two layers plays a crucial role in the persistence of oil. At locations where the seaward flow was small, the water table dropped into the lower layer, and subsequently, oil floating on it entered the lower layer and remained entrapped there due to capillary forces. At locations where the seaward flow was high, the water table during low tide did not drop into the lower layer, and the oil floating on it remained in the upper layer, and eventually got washed out to sea due to the high permeability of the upper layer.

It is still a mystery as to why the bioremediation conducted on the beach EL-056C did not successfully prevent the oil from persisting in the beach. In order to quantify the beach groundwater hydraulics, and to analogize the tidal effects on transport and resident time of nutrient applied for oil bioremediation in the beach, all of which are closely related to the oil-persistence in beaches, a tracer study was conducted using lithium as a conservative tracer on the beach EL-056C. The design of the tracer application is an analog to the nutrient application for oil bioremediation of oil polluted beaches proposed by Li et al. (2007). The tracer solution was lithium nitrate solution and was applied equally and simultaneously onto two transects of the beach. The left (facing landward) transect is clean and the right transect contains oils at the amount considered as heavy oil residue (HOR) as defined in Gibeaut and Piper (1998). The water table, the pore water concentrations of

* Corresponding author at: Dept. of Civil and Environmental Engineering, Temple University, 1947 N. 12th Street, Philadelphia, PA 19122, USA. Tel.: +1 215 204 7871; fax: +1 215 204 4696.

E-mail addresses: hailongli@cugb.edu.cn (H. Li), boufadel@temple.edu (M.C. Boufadel).

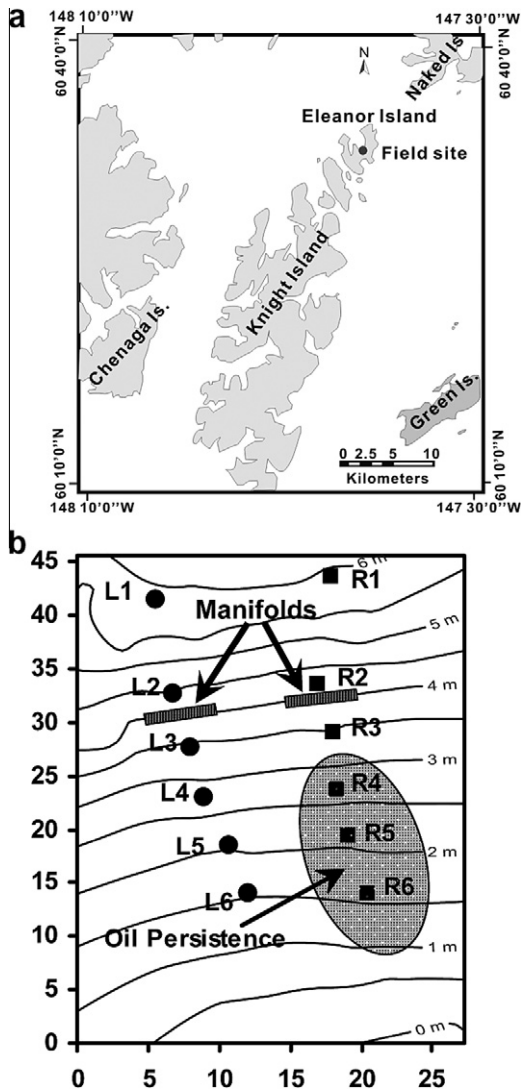


Fig. 1. (a) Location of the beach EL-056C (filled circles); (b) beach topographical contours, layout of observation wells and lithium tracer application manifolds. The elevation datum (0.0 m) is the low tide line during spring tides. All dimensions are in meter. Well names are marked with "L" for the left transect (as one stands landward on the beach) and with "R" for the right. Subsurface oil residues were found at locations R4, R5 and R6 in summer of 2007.

salinity (TDS) and lithium in the variably-saturated beach aquifer were observed during the tracer study. The results of the observations and 2-dimensional numerical simulations of the water table and pore water salinity have been reported in Li and Boufadel (2010). Here we report and analyze the results of the tracer concentration. Our goal herein is to better understand the hydrodynamics within the beach and how it affected the persistence of oil in the beach. We also discussed the implications of the tracer study for the effects of bioremediation on the oil degradation. An attempt was made to explain why the bioremediation conducted on the beach EL-056C did not successfully prevent the oil from persisting.

The layout of the paper is as follows: first the background information of the field work is given such as the study site, the tracer experiment and field measurements. Then the details for the numerical simulations are introduced, which include the numerical model, simulation domain, model parameters, boundary and initial conditions, and numerical simulation results when considering the disturbance of the beach sediments during installation of the observation wells. Finally, we numerically simulated the same

tracer experiment in the intact beach (i.e., without any beach sediment disturbance). Then the results are used to discuss the reasons for the long-term persistence of the oil spills in the beach, and the effects of bioremediation on the oil degradation.

2. Field work

2.1. Study site

The beach EL-056C is a single pocket beach with an along-shore width of only 60 m and across-shore length of 50 m. The original 1989 shoreline cleanup assessment team (SCAT) survey (Taylor and Reimer, 2008) data indicated that initial oiling at this beach was in form of continuous oil pools, with mousse and fluid oil documented to depths greater than 30 cm (Owens et al., 2008). Tides in Prince William Sound have a very large range: ~ 5 m during spring tides and ~ 2.6 m during neap tides.

2.2. Tracer study

The tracer study was conducted on two transects of the beach (see Fig. 1b, Fig. 2a and b) in summer of 2007. The left transect was clean (no oil) and the right transect was heavily oiled. The distance between the two transects was around 10 m. Lithium in a technical grade anhydrous LiNO_3 (Cyprus Foote Mineral, Kings Mountain, NC) was used as the conservative tracer (Wrenn et al., 1997b) in a seawater solution (salinity 26.5 g/L). The lithium concentration in the solution was 360 mg/L. The tracer was used successfully in previous beach tracer studies (Wrenn et al., 1997a,b). Along each of the two transects, 1050 L of tracer solution was poured on the beach surface through small holes (diameter 2 mm, inter-hole distance 10 cm) uniformly distributed along the whole length of the manifold (PVC pipe with inner diameter of 38 mm) placed on the beach surface at the elevation of 4 m above the lowest tide line (Figs. 1 and 2). The tracer was applied during the falling tide following the highest spring tide, and started when the tidal level was about 3.39 m above the lowest tide line at 3:54 AM, July 30th 2007. The tracer application lasted for 2 h and 6 min. The highest spring tide (4.61 m above the lowest tide line) occurred at 1:50 AM, July 30th 2007. This time is taken as initial time ($t = 0$) for all the time-dependent physical parameters such as the tracer concentration and tidal level throughout this paper. The length of the manifold is 5 m. The flow rate per unit length manifold was $100 \pm 3.6 \text{ L h}^{-1} \text{ m}^{-1}$. No ponding occurred on the beach surface during tracer injection. The measurement of the tracer (Lithium) concentration began immediately at the end of the tracer injection.

2.3. Field measurements

Six pairs of well locations with similar surface elevations were chosen (Fig. 1b) along the two transects. At each well location a pit was dug down to a depth from 0.66 m to 1.17 m, and then a whole-length-slotted PVC pipe and a multiport sampling well were installed vertically. A pressure transducer (MiniDiver, Data Logger-DL501, Schlumberger) was placed at the bottom of the PVC pipe to provide the water pressure every 10 min. The readings of the pressure transducer were compensated for the barometric pressure monitored by an air-pressure sensor (BaroLogger, DL-500, Schlumberger) during the same period. No rains or strong winds occurred during the experiment.

The stainless-steel multiport sampling well contained 4 ports labeled A, B, C and D from the bottom up. They were covered with fine stainless-steel screen to prevent the blockage by fine sediments. The distance between any two adjacent ports is 22 cm. Each

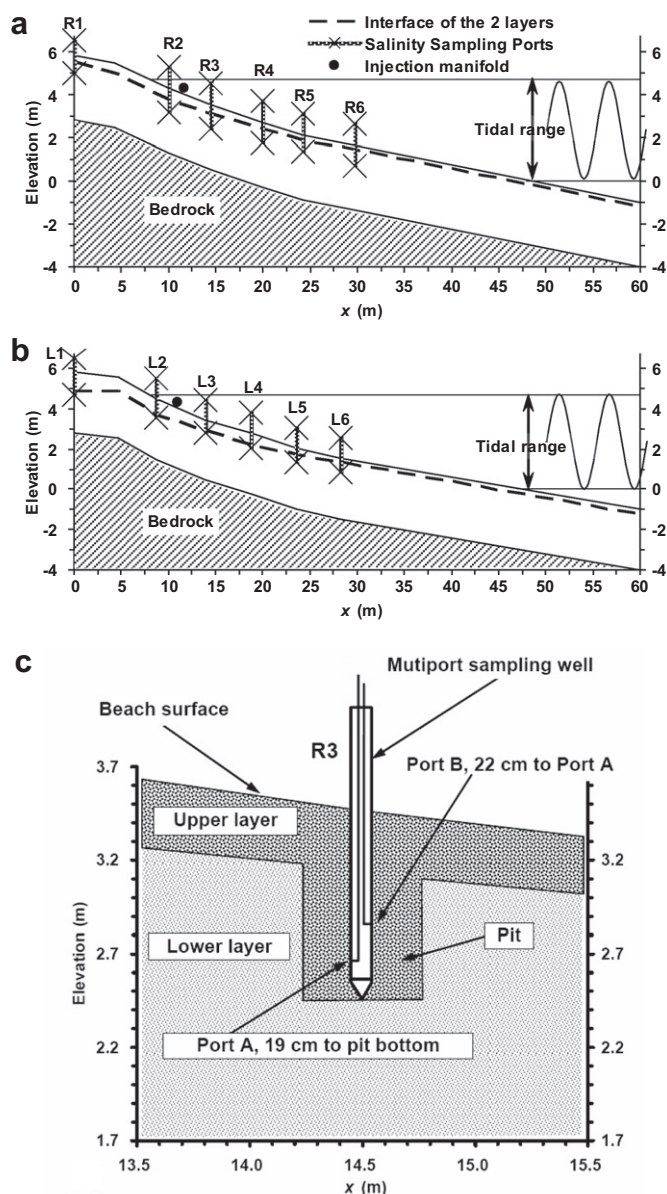


Fig. 2. Simulation domains of (a) right and (b) left transects at the beach, EL-056C. (c) The vertical cross-section of the pit at R3. Ports C and D are not shown.

port was connected to a stainless-steel tube that extended to the top of the well where it was connected through a Tygon (a brand name) tube to a three-way Luer Lock valve. Water samples (approximately 100 mL) were collected using 60-mL luer lock syringes from the multiport sampling wells and placed in 125-mL polyethylene bottles (Fischer Scientific, Fairlawn, NJ). The samples were acidified by H_2SO_4 (98%) and shipped to the laboratory at Temple University in Philadelphia, PA for chemical analysis of chlorinity and lithium concentration. Lithium concentration was measured by atomic absorption spectroscopy with an air-acetylene flame at 670.8 nm.

The chlorinity of each sample was transformed into salinity using the well-known chlorinity–salinity ratio of 19.4:35 (Duxbury and Duxbury, 2001). Using this method, salinity data were obtained for a total of 361 samples. Nineteen samples directly from the seawater near the beach gave an average seawater salinity of 26.45 g/L. Seawater salinity in Prince William Sound varies both with seawater depth and temperature. According to Coyle and Pinchuk (2005), salinity of shallow seawater varies seasonally and is

26.2 ± 0.8 g/L during the end of July and beginning of August, which is close to our salinity measurement. More details about the field measurements can be found in Li and Boufadel (2010).

3. Numerical simulations

3.1. Numerical model

Numerical simulations were conducted using the two-dimensional finite element model MARUN (Boufadel et al., 1999b). Taking into account the effects of salt concentration on fluid density and viscosity, MARUN is able to simulate groundwater flow of two-component (one is salt and another could be nutrients or tracer) in variably-saturated porous media. The variable pore water saturation, the relative permeability and the capillary pressure were described by the van Genuchten (1980) model. Boufadel et al. (1999c) verified the MARUN code by reproducing previous well-known numerical results such as the Henry's problem of seawater intrusion (Frind 1982) and the Elder problem (Elder, 1967). The MARUN code was also validated extensively in the literature (e.g., Boufadel, 2000; Naba et al., 2002; Guo et al. 2010; Li et al., 2007, 2008; Li and Boufadel, 2010; Xia et al., 2010) via predicting laboratory and field experiment data. Model equations for the groundwater flow, the solute and tracer transports are given in details in Xia et al. (2010). Because the groundwater flow within the beach is mainly cross-shore, the 5 m long manifold for tracer application may adequately mitigate the along-shore dispersion of the applied tracer so that the two-dimensional numerical model is able to describe the groundwater flows and tracer transportations along the two transect with adequate accuracy. This has been demonstrated by the numerical simulation results of MARUN to the similar tracer study at another beach (Xia et al., 2010).

3.2. Simulation domains

Two simulation domains were chosen for the right and left transects, respectively. Both domains have a uniform thickness of 3 m and horizontal extent of 60 m (Fig. 2a and b). Field investigation, water table observation and numerical simulations indicated that the beach sediments can be conceptually modeled as two piecewise homogeneous layers: a permeable upper layer of coarse, loose material and a much less permeable lower layer with compacted fine material (Li and Boufadel, 2010). The thicknesses of the upper layer at selected locations are listed in Table 1.

During installation of the observation wells in each pit, the original compacted/consolidated, less permeable material in the lower layer was replaced by the loosened, mixed materials from the surface and lower layers. This significantly enhanced the permeability in the pit (referred to as pit effect hereafter), which should be considered in modeling the field observations (Fig. 2c). In our simulations, a zone of the same permeability as the upper layer was assigned to the pits. The zone had a horizontal bottom of 0.3–0.6 m wide and 0.19 m lower than the elevation of the deepest sampling port (see Table 1 and Fig. 2c). The same method was also successfully used to describe the pit effect in the numerical model for the beach groundwater flow and solute transport in other beaches (e.g., Xia et al., 2010; Guo et al. 2010).

3.3. Model parameters

Model parameter values used in the simulation are summarized in Table 2.

The upper layer comprises loose, coarse material with negligible capillary effects. In order to approximate the negligible capillary effects, relatively large values were chosen for the van Genuchten

Table 1
Elevation of beach surface and thickness of the upper layer at different locations along the right and left transects (after Li and Boufadel (2010)).

Locations	x (m)	Surface elevation z (m)	Thickness of surface layer (m)	Depth of the deepest port (m)
R1	0	5.83	0.33	0.66
R*1	4.3	5.48	0.5	N/A
R2	10.1	4.31	0.55	0.97
R3	14.5	3.5	0.4	0.92
R4	20	2.73	0.3	0.76
R5	24.3	2.09	0.2	0.55
R6	29.7	1.62	0.1	0.7
R*2	60.0	-1.00	0.1	N/A
L1	0.00	5.83	0.98	0.98
L*1	4.73	5.56	0.70	N/A
L2	8.75	4.48	0.80	0.73
L3	13.95	3.45	0.52	0.47
L4	18.71	2.78	0.55	0.57
L5	23.55	2.04	0.3	0.49
L6	28.32	1.53	0.20	0.47
L*2	60.0	-1.00	0.20	N/A

Locations R*1, R*2, L*1 and L*2 are only used to control the geometry of the surface and interfaces, no wells were installed at these locations. R*2 and L*2 are the seaward boundaries of right and left transects, respectively. "N/A" means not available.

Table 2
Model parameter values used in the numerical simulations (after Li and Boufadel (2010)).

Symbol	Definition	Dimension	Value
α	Sand capillary fringe parameter of the van Genuchten model	1/m	40 (upper layer) 0.5 (lower layer)
α_l	Longitudinal dispersivity	m	0.1
α_r	Transverse dispersivity	m	0.01
K	Hydraulic conductivity for saturated freshwater	m/s	10^{-2} (upper layer) 10^{-5} (lower layer)
n	Sand grain size distribution parameter of the van Genuchten model	-	7.0 (upper layer) 2.0 (lower layer)
S_r	Residual soil saturation	-	0.01
ϕ	Porosity	-	0.30
τD_m	Molecular diffusion coefficient in porous media	m^2/s	10^{-9}
	Seawater–freshwater density ratio	-	1.0202
	Seawater salinity	g/L	26.5

parameters ($\alpha = 40 \text{ m}^{-1}$ and $n = 7$) in the upper layer. Other model parameter values used are: saturated water content ($0.3 \text{ m}^3/\text{m}^3$), residual water content ($0.01 \text{ m}^3/\text{m}^3$), molecular diffusion coefficient ($10^{-9} \text{ m}^2/\text{s}$) based on chloride diffusion in pure water (Schulz, 2000), seawater salinity (26.5 g/L), seawater–freshwater density ratio (1.0202) which was calculated by the method of Fofonoff and Millard (1983) based on the in situ average temperature ($12 \text{ }^\circ\text{C}$) and barometric pressure (103.7 kPa).

3.4. Boundary and initial conditions

The tracer injection was simulated by specified water flow rate and concentrations of salt and tracer during the injection at the boundary node (injection node) on the beach surface closest to the manifold (see Fig. 2a and b). Zero-flow and zero-mass transport boundary conditions were used along the domain bottom and beach surface above the tidal level (except the injection node during tracer injection). At the landward boundary the water level was fixed at 5.15 m and the salinity was fixed at 0.0 g/L based on the water level and salinity observations at L1 and R1. On the sub-

Table 3
Tidal parameter values.

Harmonic component i	Amplitude A_i (m)	Phase shift φ_i (rad)	Explanations
1	-0.42167	-0.1357	Main lunar diurnal (O1), $\omega_1 = 0.243351885 \text{ rad/h}$
2	-0.5852	-0.4538	Lunar–solar diurnal (K1), $\omega_2 = 0.262516177 \text{ rad/h}$
3	1.3162	1.3061	Main lunar semidiurnal (M2), $\omega_3 = 0.505868017 \text{ rad/h}$
4	0.4533	2.6425	Main solar semidiurnal (S2), $\omega_4 = 0.523598776 \text{ rad/h}$
5	-0.0269	2.7968	Lunar elliptic (N2), $\omega_5 = 0.496366928 \text{ rad/h}$

merged beach surface and sea-floor, the water pressure was equal to the tidal seawater column above the beach surface and the salinity was flow-direction dependent with constant seawater concentration where flow was inward, zero concentration gradient where flow was outward. Tidal moving boundary condition was used in the sense that the submerged portion of the beach surface was updated at each time step by comparing the tidal level and the beach surface elevation. A schematic diagram for the boundary conditions was given in Supplementary Information of Li and Boufadel (2010).

Following Li and Boufadel (2010), the tidal level H_{Tide} is represented by the analytical expression:

$$H_{\text{Tide}}(t) = h_{\text{MSL}} + \sum_{i=1}^5 A_i \cos(\omega_i t + \varphi_i) \quad (1)$$

where h_{MSL} is the mean sea level (equaling 2.49 m), A_i , ω_i and φ_i are the amplitude, frequency [LT^{-1}] and phase shift (in radian) of the i th component of the tides, respectively. Five harmonic components (O1, K1, M2, S2 and N2) are included since they account for approximately 95% of the tidal potential (Melchior, 1964; Merritt, 2004). The parameters A_i , ω_i and φ_i were estimated using the least-squares fitting to the water level observed at the most seaward well in the beach (Well L6 and R6) when the ground surface of the wells were submerged by seawater. Their values were listed in Table 3. The tidal level predicted by Eq. (1) is reported in Fig. 3. The datum of the water level is the low tide line during the spring tides.

The simulation started from a hydrostatic initial condition at low tide with a sharp freshwater–seawater interface approximated by the well-known Ghyben–Herzberg approximation (Freeze and Cherry, 1979). To obtain quasi-steady state numerical solution, the simulation was run about 20 spring–neap tidal cycles until the difference of the water table and the difference of the salinity between two successive spring–neap tidal cycles became negligible. Then the tracer injection was simulated. The variable time step was constrained by a Courant number less than 0.90. The mesh was made fine enough (mesh resolution of $\sim 0.10 \text{ m}$, 31 nodes along the 3.0 m depth, and 543 nodes along the 60 m cross-shore length) to meet the strict criterion for the grid Péclet number to be less than or equal to 2.0 (Zheng and Bennett, 2002).

4. Results

Our numerical simulations of density-coupled groundwater flow and salt transport model reproduced the observed water table, salinity, and lithium concentration in both transects. The results of water table and salinity have been shown and discussed in Li and Boufadel (2010). Here we focus on the lithium concentration. The time series of the observed and simulated lithium concentrations at different ports are shown in Fig. 3 together with the tidal level variations predicted by Eq. (1). The following obser-

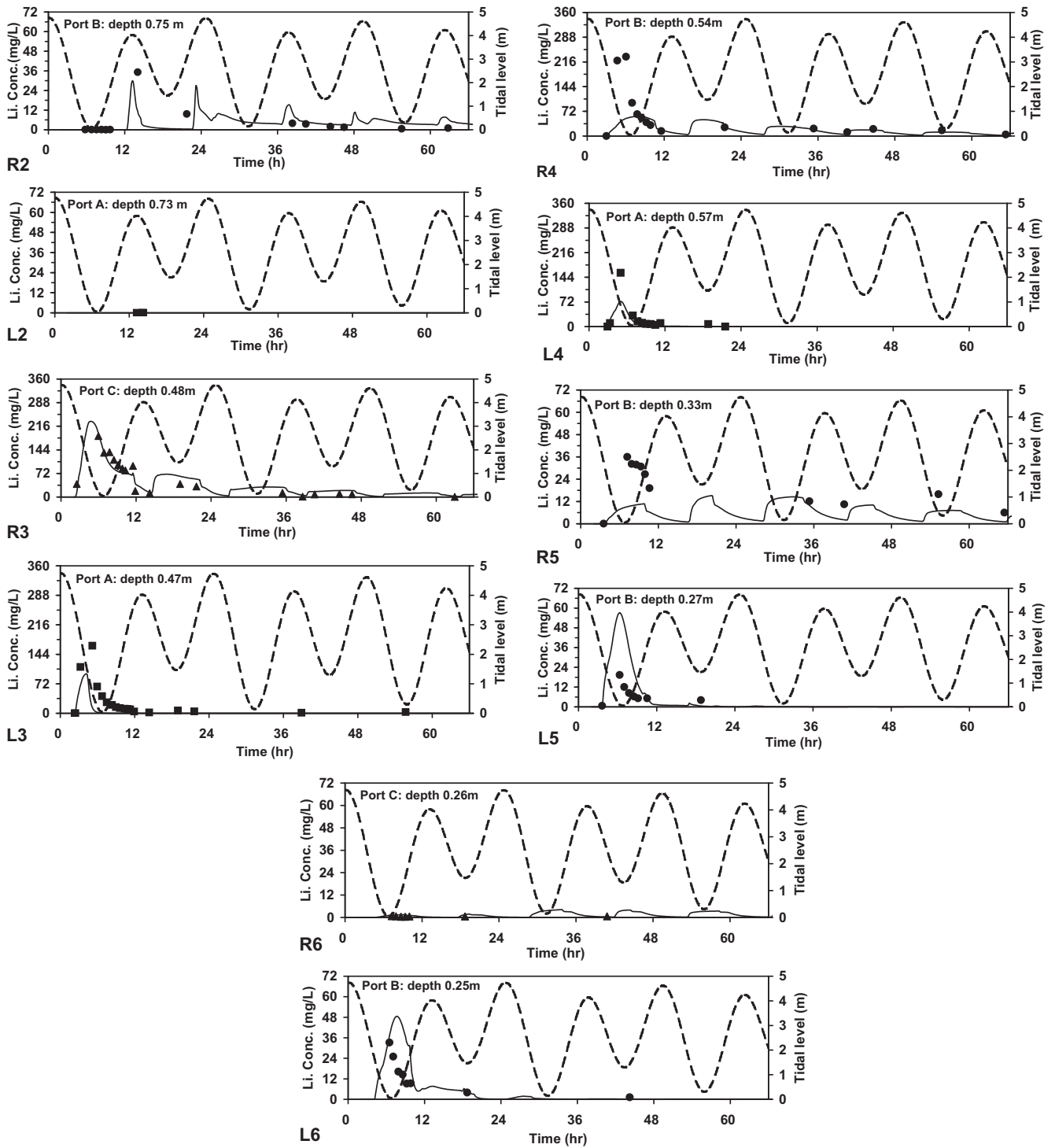


Fig. 3. Observed (symbols) and simulated (solid lines) lithium concentration of the pore water at selected pair of ports at L2 and R2, L3 and R3, L4 and R4, L5 and R5, and L6 and R6. The tidal level variation with time (dashed line) is also shown using the right vertical axis. The initial time ($t = 0$) is 1:50 AM, July 30th 2007 when the spring high tide occurred. The 2.1-h long seawater lithium tracer injection started at $t = 2.06$ h. In each panel, observed and simulated results only from one port are shown, with the port depth from the beach surface indicated there. For the sake of convenience for comparisons between the two transects, the ports are selected so that the depths of each pair of ports are as close as possible.

variations can be made from Fig. 3. Along the right transect, the match between the simulation and observation is very good at port in R3 and became gradually worse seaward, albeit more or less acceptable. Fig. 3 also indicated that at L2 of the left transect, both the simulated and observed lithium concentrations are zero (The simulated lithium concentration is zero and coincident with the

abscissa). The match between the simulation and observation is good at L3 and became a little bit worse for other wells (L4, L5 and L6). The error may be caused by the local heterogeneity of the beach sediments.

Despite the errors between the simulation and observation results, the simulation results captured the following main features

of the observations of the groundwater flow and tracer transport along the two transects:

- (1) The observation showed that the lithium was flooded into R2, but not into L2 by the high tide following the tracer injection, our simulation results reproduced these facts (see R2 and L2 of Fig. 3, as well as Fig. 4b).
- (2) At every well of the left transect the time series of observed lithium concentration had only one peak and approached zero within 24 h, but at most wells of the right transect it had multi-peaks (see R3, R4 and R5 of Fig. 3, at R2 and R6 the lithium concentration data were too sparse to demonstrate the multi-peaks). Our simulated results reproduced this difference between the two transects.
- (3) The lithium stayed much longer within the right transect than within the left transect. This can be seen from comparison between, e.g., R4 and L4 in Fig. 3: while at R4 there was still considerable lithium (both observed and simulated) around $t = 56$ h, at L4 there was no lithium after $t = 12$ h. Similar comparisons can be made between the pairs of R5 and L5, R6 and L6, R3 and L3, and R2 and L2. Spatial distributions of lithium within the two transects at different times give clearer description of this fact. At the first low tide after the injection (Fig. 4a) the front the lithium (18 mg/L contour line) arrived at $x = 35$ m in the left transect but only at about $x = 21$ m in the right transect. At the first high tide after the injection (Fig. 4b) a considerable lithium mass (concentration >18 mg/L) arrived at R2 ($x = 10$ m) in the right transect but no lithium reached L2 ($x = 10$ m) in the left transect. At the second low tide after the injection, most of the lithium plume persisted in the middle-high intertidal zone in the right transect but that in the left transect was washed out to the sea (Fig. 4c).

5. Discussions

The numerical simulations and analyses above included the pit effect. However, the oil spills and the nutrient application for the oil bioremediation occurred in the intact beaches (namely, without the pit effect as described in Fig. 2c). In order to investigate the groundwater flow and nutrient transport in the intact beach, we conducted numerical tracer simulations without pits, with the model configuration and model parameters, and as well as the tracer injection procedure unchanged. These simulations are expected to tell us what will happen if nutrients or tracer is injected in a beach without pits.

Fig. 5 shows the simulated groundwater flow velocity and contours of lithium concentration within the right and left transects of the intact beach (without pits) at different times. There were large differences in the groundwater flow and solute transport between the left and right transects of the intact beach. One can see that the seaward groundwater flow near the water table was around one order of magnitude larger along the left transect than along the right transect, indicating that the fresh groundwater flow from inland is larger in the left transect than in the right one. The tracer was washed out to the sea much more quickly along the left transect than along the right transect.

If the lithium concentration can be viewed as surrogate for oil, the above simulation results may also be used to explain why the subsurface oil persistence happens within the lower layer of the right transect but not within the left transect. During the initial oiling stage, there were a lot of oils on the beach surface which might penetrate into the upper layer of the whole beach. The oils entering the upper layer stayed much longer before they were washed back to the sea along the right transect than along the left transect, providing much more opportunities for oils in the upper layer to penetrate into the lower layer along the right transect than

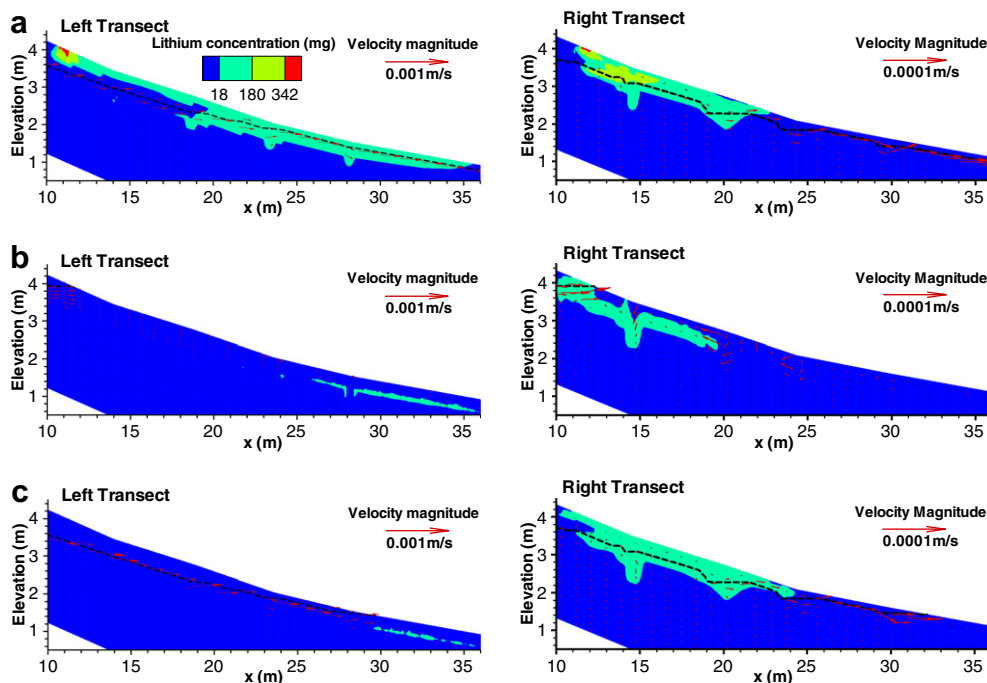


Fig. 4. Simulated spatial lithium concentration distributions and water table (Black dashed lines) of the right and left transects at different times. The pit effect was considered. (a) At first low tide after the tracer injection ($t = 7.0$ h), (b) at first high tide after the tracer injection ($t = 13.5$ h), and (c) at second low tide after the tracer injection ($t = 19.0$ h). The initial time ($t = 0$) is 1:50 AM, July 30th 2007 when the spring high tide occurred. The 2.1-h long lithium tracer injection started at $t = 2.06$ h. The lithium concentration of the tracer solution is 360 mg/L. The three lithium concentration contours represent 5% (18 mg/L), 50% (180 mg/L) and 95% (342 mg/L) of the concentration of tracer solution, respectively. Note that the scale of the velocity magnitude for the left transect is 10 times of that of the right transect.

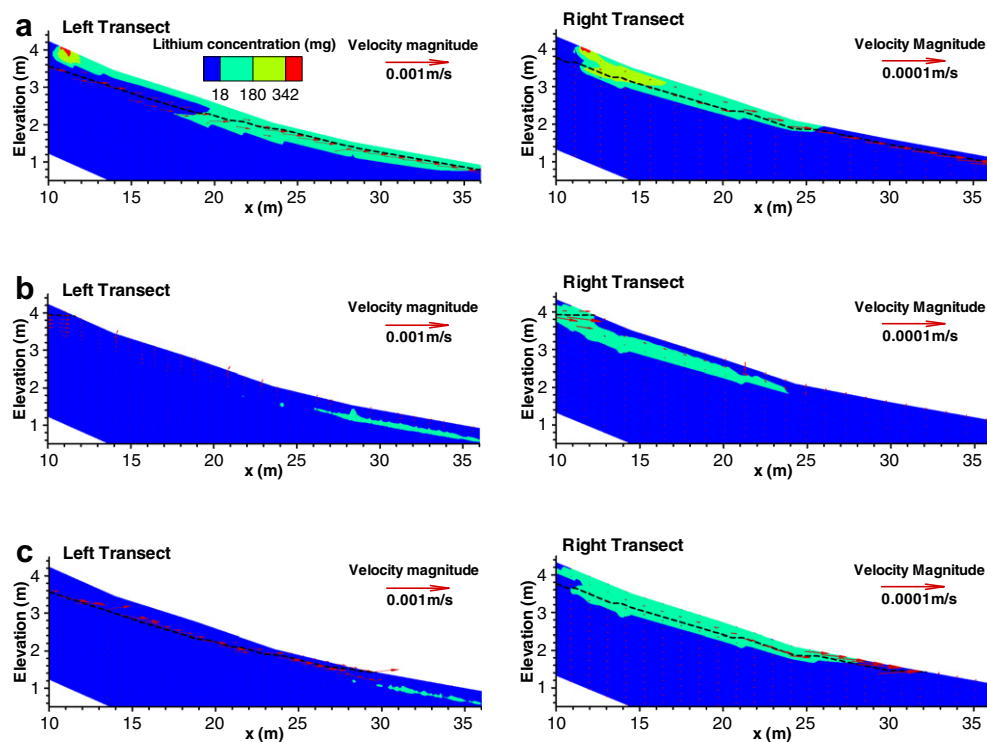


Fig. 5. Simulated spatial tracer concentration distributions (color contours) and water table (black dashed lines) of the right and left transects of the intact beach (without pits) at different times. (a) At first low tide after the tracer injection ($t = 7.0$ h), (b) at first high tide after the tracer injection ($t = 13.5$ h), and (c) at second low tide after the tracer injection ($t = 19.0$ h). The initial time ($t = 0$) is 1:50 AM, July 30th 2007 when the spring high tide occurred. The 2.1-h long lithium tracer injection started at $t = 2.06$ h. The tracer concentration is 360 mg/L. The three lithium concentration contours represent 5% (18 mg/L), 50% (180 mg/L) and 95% (342 mg/L) of the concentration of tracer solution, respectively. Note that the scale of the velocity magnitude for the Left Transect is 10 times of that of the right transect.

along the left transect, and resulting in the persistence of oil in the lower layer of the right transect. Of course, this explanation is valid only qualitatively since the oil–water two-phase flow during the initial oiling stage could not be quantitatively described by the tracer transport here. A more direct application of the tracer study is in the context of oil biodegradation, as described next.

Prior bioremediation studies were conducted on this beach in 1989, 1991, and 1992 (Bragg et al., 1994; Taylor and Reimer, 2008). We are also contemplating an additional bioremediation study in the coming years. Laboratory and field studies of bioremediation indicated that nitrogen concentration between 2.0 mg/L and 10.0 mg/L is sufficient for near-maximum growth of hydrocarbon-degrading microorganisms (Boufadel et al., 1999a; Venosa et al., 1996; Venosa and Zhu, 2003; Wrenn et al., 2006). Thus the lack of its biodegradation was probably due to limitations of nutrients and/or dissolved oxygen within the oiled transect. If it is hypothesized that the decreasing of the applied nutrient in the beach is caused mainly by the tidal flushing and washing, not by the microbial uptake, one could use our tracer study as surrogate for nutrient application on the beach for the purpose of bioremediation. Owing to the linear dependence of the pore water nutrient concentration on the nutrient solution applied, the contours of 18 mg/L, 180 mg/L and 342 mg/L in Fig. 5, which resulting from a source concentration of 360 mg/L, can be viewed as 2 mg/L, 20 mg/L and 38 mg/L for a source concentration of nutrient of 40 mg-N/L, respectively. In this case, the simulated tracer spatial distribution in Fig. 5 indicated that the nutrient applied along the left transect would be washed to the sea very quickly (within less than one tidal cycle) by the relatively large freshwater flow from inland. This implies that the nutrient application has very limited effects on the degradation of the oil spills in the left transect, or equivalently, the reason for the left transect to be clean was due to factors other than bioremediation. This supports independently,

though indirectly, the conclusion by Li and Boufadel (2010) that the clean left transect is mainly due to the high water table located in the upper layer which acted as a barrier to the downward penetrating of the oil spills in the upper layer. Oil spills in the upper layer could not persist due to the high permeability of that layer.

The nutrient plume in the right transect stayed a long time in the beach and a major part of it entered the lower layer. This fact implies that the bioremediation along this transect was not limited by the lack of nutrients. However, subsurface oil that is only slightly weathered persists within the lower layer of this transect (Li and Boufadel, 2010), which implies that the bioremediation or the degradation of the subsurface oil spill was essentially hampered by factors other than the nutrients. Thus, we reach the same conclusion of Li and Boufadel (2010) that the subsurface oil persistence was due to the lack of oxygen based on the data of tracer study, which is independent of the data of the water table and pore water salinity used in Li and Boufadel (2010).

Fig. 6a shows how the masses of the lithium tracer in the upper layer along the left and right transects change with time during and after the tracer injection. The tracer mass in the upper layer of the left transect decreased to around 5 g within 10 h after the injection and became essentially zero after $t = 36$ h with a slight fluctuation. In contrast, the tracer mass in the upper layer of the right transect fluctuated with the tides significantly, and decreased very slowly and remained around 5 g even at $t = 72$ h. Fig. 6b shows how the masses of the lithium tracer in the lower layer along the left and right transects change with time during and after the tracer injection. For the left transect, the tracer mass decreased quickly and monotonically from the peak of near 40 g after the injection to around 5 g when $t = 36$ h. In contrast, the tracer mass in the lower layer of the right transect fluctuated with the tide significantly, and decreased very slowly and remained around 20 g even at $t = 80$ h. These observations confirm again the above con-

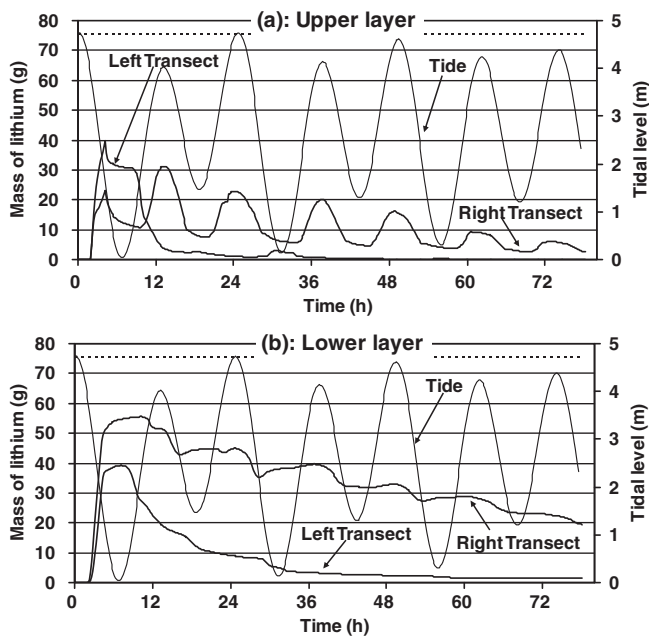


Fig. 6. Variations of the lithium mass within (a) the upper layer, and (b) the lower layer with time during and after the tracer injections along the right and left transects. The total lithium mass injected along each transect is 75.6 g (indicated in dashed line). The tidal level is shown using the right vertical axis. Note that the lithium stayed much longer within the right transect than within the left transect. In addition, in each transect, the lithium stayed longer in the lower layer than in the upper layer.

clusions about the quick washout of nutrients within the left transect and the long stay of the nutrients within the right transect.

6. Conclusions

The 1989 Exxon Valdez oil spills persist in the subsurface of some gravel beaches in Prince William Sound, Alaska, despite the bioremediations conducted in summers from 1989 to 1992. This paper reports a tracer study using lithium on a gravel beach and its implications for the oil persistence. Lithium nitrate solution was applied equally and simultaneously onto two transects of the beach. The left (facing landward) transect was clean and the right transect contained Heavy Oil Residue that is only slightly-weathered. The tracer injections and transports along the two transects were modeled using the 2-dimensional cross-sectional numerical model MARUN (Boufadel et al., 1999b). Model results faithfully reproduced the tracer concentrations observed at 10 wells along the two transects. The results show that the residence time of the tracer in the oiled, right transect was several times longer than that in the clean, left transect due to the smaller inland groundwater recharge into the right transect. If the tracer is regarded as oils, the results imply that the oils would stay several times longer within the right transect than within the left transect, providing much more opportunities for the oils in the upper layer to enter the lower layer in the right transect than in the left one. This may explain, at least qualitatively, why oil persistence happens within the right but not within the left transect. If the tracer is regarded as nutrients, the results imply that the nutrients would stay several times longer within the right, oiled transect than within the left, clean transect. This indicated that the oil persisting in the lower layer of the right transect was not due to the lack of nutrients during the bioremediation since the nutrients added on this transect would stay long enough within the beach before they

were washed back to the sea. Similarly, the reason for the left transect to be clean was due to factors other than bioremediation since the nutrients added on this transect would be quickly washed back to the sea. These understandings add new insights into the roles played by groundwater hydraulics and bioremediations in determining the fate of oil spills in beaches.

Acknowledgements

This work was supported by the Exxon Valdez Oil Spill Trustee Council (No. 070836). However, it does not necessarily reflect the views of the Council, and no official endorsement should be inferred. H.L. thanks the NSFC (National Natural Science Foundation of China) Outstanding Young Scientist Grant (No. 41025009). The authors thank the editor and an anonymous reviewer for their thoughtful comments.

References

- Boufadel, M.C., 2000. A mechanistic study of nonlinear solute transport in a groundwater–surface water system under steady state and transient hydraulic conditions. *Water Resources Research* 36 (9), 2549–2565.
- Boufadel, M.C. et al., 1999a. Optimal nitrate concentration for the biodegradation of *n*-heptadecane in a variably-saturated sand column. *Environmental Technology* 20, 191–199.
- Boufadel, M.C., Suidan, M.T., Venosa, A.D., 1999b. A numerical model for density- and viscosity-dependent flows in two-dimensional variably-saturated porous media. *Journal of Contaminant Hydrology* 36 (1–2), 1–20.
- Boufadel, M.C., Suidan, M.T., Venosa, A.D., Bowers, M.T., 1999c. Steady seepage in trenches and dams: effect of capillary flow. *Journal of Hydraulic Engineering ASCE* 125 (3), 286–294.
- Bragg, J.R., Prince, R.C., Harner, E.J., Atlas, R.M., 1994. Effectiveness of bioremediation for the Exxon Valdez oil spill. *Nature* 368, 413–418.
- Coyle, K.O., Pinchuk, A.I., 2005. Seasonal cross-shelf distribution of major zooplankton taxa on the northern Gulf of Alaska shelf relative to water mass properties, species depth preferences and vertical migration behavior. *Deep Sea Research Part II: Topical Studies in Oceanography* 52 (1–2), 217–245. doi:10.1016/j.dsr2.2004.09.025.
- Davies, J.L., 1980. *Geographical Variation in Coastal Development*, second ed. Longman, London. 224 pp.
- Duxbury, A.B., Duxbury, A.C., 2001. *Fundamentals of Oceanography*. McGraw-Hill, New York.
- Elder, J.W., 1967. Transient convection in a porous medium. *Journal of Fluid Mechanics* 27, 609–623.
- Fofonoff, N.P., Millard, R.C., 1983. Algorithms for computation of fundamental properties of seawater, UNESCO Technical Paper in Marine Science 44, UNESCO.
- Freeze, R.A., Cherry, J.A., 1979. *Groundwater*. Prentice Hall, Englewood Cliffs, NJ. 604 pp.
- Frind, E.O., 1982. Simulation of long-term transient density-dependent transport in groundwater. *Advanced in Water Resources* 5, 73–88.
- Gibeaut, J.C., Piper, E., 1998. 1993 Shoreline Oiling Assessment of the Exxon Valdez Oil Spill; EVOS Restoration Project Final Report 93038, Exxon Valdez Trustee Council, Anchorage, AK.
- Guo, Q., Li, H., Boufadel, M.C., Sharifi, Y., 2010. Hydrodynamics in a gravel beach and its impact on the Exxon Valdez oil. *Journal of Geophysical Research* 115, C12077. doi:10.1029/2010JC006169.
- Hayes, M.O., 1967. Relationship between coastal climate and bottom sediment type on the inner continental shelf. *Marine Geology* 5, 111–132.
- Hayes, M.O., Michel, J., 1999. Factors determining the long-term persistence of Exxon Valdez oil in gravel beaches. *Marine Pollution Bulletin* 38, 92–101.
- Li, H.L., Boufadel, M.C., 2010. Long-term persistence of oil from the Exxon Valdez spill in two-layer beaches. *Nature Geoscience* 3 (2), 96–99. doi:10.1038/ngeo749.
- Li, H.L., Zhao, Q.H., Boufadel, M.C., Venosa, A.D., 2007. A universal nutrient application strategy for the bioremediation of oil polluted beaches. *Marine Pollution Bulletin* 54, 1146–1161.
- Li, H.L., Boufadel, M.C., Weaver, J.W., 2008. Tide induced seawater–groundwater circulation in shallow beach aquifer. *Journal of Hydrology* 352 (1–2), 211–224. doi:10.1016/j.jhydrol.2008.01.013.
- Melchior, P., 1964. In: Odishaw, H. (Ed.), *Earth tides in Research in Geophysics*, v.2. Massachusetts Institute of Technology Press, Cambridge, MA, pp. 183–193.
- Merritt, M.L., 2004. Estimating hydraulic properties of the Floridian aquifer system by analysis of earth-tide, ocean-tide, and barometric effects, Collier and Hendry Counties, Florida. *Water Resources Investigations Report 03-4267*, United States Geological Survey, Tallahassee, FL.
- Michel, J., Hayes, M.O., 1999. Weathering patterns of oil residues eight years after the Exxon Valdez oil spill. *Marine Pollution Bulletin* 38 (10), 855–863.
- Naba, B., Boufadel, M.C., Weaver, J.W., 2002. The role of capillary forces in steady-state and transient seepage flows. *Ground Water* 40 (4), 407–415.

- Neff, J.M., Owens, E.H., Stoker, S.W., McCormick, D.M., 1995. Shoreline oiling conditions in Prince William Sound following the “Exxon Valdez” oil spill. In: Wells, P.G., Butler, J.N., Hughes, J.S. (Eds.), *Exxon Valdez Oil Spill–Fate and Effects in Alaskan Waters*. ASTM STP 1219 American Society for Testing and Materials, Philadelphia, PA, pp. 312–346.
- Owens, E.H., Taylor, E., Humphrey, B., 2008. The persistence and character of stranded oil on coarse-sediment beaches. *Marine Pollution Bulletin* 56 (1), 14–26.
- Schulz, H.D., 2000. Quantification of early diagenesis: dissolved constituents in marine pore water. In: Schulz, H.D., Zabel, M. (Eds.), *Marine Geochemistry*. Springer, Berlin, Heidelberg, New York.
- Short, J.W., Lindeberg, M.R., Harris, P.M., Maselko, J.M., Pella, J.J., Rice, S.D., 2004. Estimate of oil persisting on the beaches of Prince William Sound 12 years after the Exxon Valdez oil spill. *Environmental Science and Technology* 38 (1), 19–25.
- Short, J.W., Maselko, J.M., Lindeberg, M.R., Harris, P.M., Rice, S.D., 2006. Vertical distribution and probability of encountering intertidal Exxon Valdez oil on shorelines of three embayments within Prince William Sound, Alaska. *Environmental Science and Technology* 40 (12), 3723–3729.
- Short, J.W., Irvine, G.V., Mann, D.H., Maselko, J.M., Pella, J.J., Lindeberg, M.R., Payne, J.R., Driskell, W.B., Rice, S.D., 2007. Slightly weathered Exxon Valdez oil persists in Gulf of Alaska beach sediments after 16 years. *Environmental Science and Technology* 41 (4), 1245–1250.
- Taylor, E., Reimer, D., 2008. Oil persistence on beaches in Prince William Sound – a review of SCAT surveys conducted from 1989 to 2002. *Marine Pollution Bulletin* 56, 458–474.
- van Genuchten, M.T., 1980. A closed-form equation for predicting the hydraulic conductivity of unsaturated soils. *Soil Science Society of America Journal* 44 (5), 892–898.
- Venosa, A.D., Zhu, X.Q., 2003. Biodegradation of crude oil contaminating marine shorelines and freshwater wetlands. *Spill Science and Technology Bulletin* 8 (2), 163–178.
- Venosa, A.D., Suidan, M.T., Wrenn, B.A., Strohmeier, K.L., Haines, J., Eberhart, B.L., King, D., Holder, E., 1996. Bioremediation of an experimental oil spill on the shoreline of Delaware Bay. *Environmental Science and Technology* 30, 1764–1775.
- Wrenn, B.A., Boufadel, M.C., Suidan, M.T.S., Venosa, A.D., 1997a. Nutrient transport during bioremediation of crude oil contaminated beaches, Fourth International Symposium on In-situ and On-site Bioremediation. Batelle Press, New Orleans, LA. pp. 267–272.
- Wrenn, B.A., Suidan, M.T., Strohmeier, K.L., Eberhart, B.L., Wilson, G.J., Venosa, A.D., 1997b. Nutrient transport during oil-spill bioremediation: evaluation with lithium as a conservative tracer. *Water Research* 31 (3), 515–524.
- Wrenn, B.A., Sarnecki, K.L., Kohar, E.S., Lee, K., Venosa, A.D., 2006. Effects of nutrient source and supply on crude oil biodegradation in continuous-flow beach microcosms. *Journal of Environmental Engineering ASCE* 132, 75–84.
- Xia, Y., Li, H., Boufadel, M.C., Sharifi, Y., 2010. Hydrodynamic factors affecting the persistence of the Exxon Valdez oil in a shallow bedrock beach. *Water Resources Research*, 46, W10528, doi: 10.1029/2010WR009179.
- Zheng, C., Bennett, G.D., 2002. *Applied Contaminant Transport Modelling*. John Wiley and Sons, New York, USA.